

**Title:**

Supporting Information for Instantaneous Areal Population Density of Entire Atlantic Cod and Herring Spawning Groups and Group Size Distribution Relative to Total Spawning Population

**Author:**

Nicholas C. Makris <sup>1,\*</sup>, Olav Rune Godø<sup>2,5</sup>, Dong Hoon Yi <sup>1</sup>, Gavin J. Macaulay <sup>2</sup>, Ankita D. Jain <sup>1</sup>, Byunggu Cho <sup>1</sup>, Zheng Gong <sup>1</sup>, J. Michael Jech <sup>3</sup>, and Purnima Ratilal <sup>4</sup>

**Author Affiliation:**

<sup>1</sup> Center for Ocean Engineering, Massachusetts Institute of Technology, 77 Massachusetts Avenue, Cambridge MA 02139, USA

<sup>2</sup> Institute of Marine Research, Post Office Box 1870, Nordnes, N-5817 Bergen, Norway

<sup>3</sup> NOAA Northeast Fisheries Science Center, 166 Water Street, Woods Hole, MA 02543, USA

<sup>4</sup> Department of Electrical and Computer Engineering, Northeastern University, 360 Huntington Avenue, Boston, MA 02115, USA

<sup>5</sup> Christian Michelsen Research, Post Office Box 6031, N-5892 Bergen, Norway

**\* Corresponding Author:**

Name: Nicholas C. Makris

Address: Center for Ocean Engineering, Massachusetts Institute of Technology, 77 Massachusetts Avenue, Cambridge MA 02139, USA

Telephone number: 617-258-6104

Email address: makris@mit.edu

# S1 Areal population density of entire Atlantic cod spawning groups

## S1.1 Acoustic sensing methods

Two research vessels were employed to measure cod in the Nordic Seas 2014 Experiment. Both the RV Knorr and RV Johan Hjort collected vertical echosounding data along line transects. The beamwidth of the vertical echosounder deployed from RV Knorr was  $35.0^\circ$  at 12 kHz, which yields a 60-m diameter resolution footprint at 100-m depth where many of the fish groups we imaged were concentrated, while that for RV Johan Hjort was  $6.8^\circ$  at 38 kHz, which yields a 12-m diameter resolution footprint at 100-m depth.

The RV Knorr towed the OAWRS source and receiver arrays (Fig.S1) and collected OAWRS data. OAWRS images were produced by beamforming, matched filtering, and charting the received OAWRS returns and then correcting for transmission loss (Makris et al., 2006a, 2009a; Jagannathan et al., 2009; Gong et al., 2010). In the Nordic Seas 2014 Experiment, an effectively monostatic arrangement for acoustic measurements was used where the source and receiver arrays were towed by the same research vessel (Fig.S1). Linear frequency modulated (LFM) source waveform transmissions of 50 Hz bandwidth and 1 second duration centered at 955 Hz were sent every 50 seconds for the OAWRS cod measurements presented. Similar information about the Gulf of Maine 2006 herring measurements presented appear in Makris et al. (2006a) and Jagannathan et al. (2009).

## S1.2 Cod areal population density obtained by OAWRS

OAWRS cod population density distributions  $n_{A,OAWRS}(\rho_c)$  were determined from measured OAWRS intensities converted to scattering strength  $SS_{OAWRS}(\rho_c)$  at horizontal location  $\rho_c$  following the standard procedures described in Jagannathan et al. (2009), Gong et al. (2010), Makris et al. (2006a) and Makris et al. (2009a). This included averaging over 5 consecutive, instantaneous OAWRS images and two consecutive 15-m range cells to reduce the measured OAWRS intensity standard deviation to roughly 1 dB or 25 percent (Makris et al., 2009a; Jagannathan et al., 2009; Gong et al., 2010; Makris et al., 2006b, 2009b; Makris, 1996; Tran, Andrews, & Ratilal, 2012). Stochastic propagation modeling (Makris et al., 2006b, 2009b; Jain, Ignisca, Yi, Ratilal, & Makris, 2013; Gong et al., 2014) was performed to obtain expected transmission loss (Makris et al., 2006b, 2009b; Jain et al., 2013; Gong et al., 2014) as a function of  $\rho_c$ . This was done by averaging 100 parabolic equation (Collins, 1993) realizations of the waveguide intensity field each employing a unique sound speed profile measured during the Nordic Seas 2014 Experiment (Fig.S2) at 500 m increments (Chen, Ratilal, & Makris, 2005) along the propagation path. It led to a standard deviation of roughly 1 dB in transmission loss over the group thickness. Mean cod target strength  $TS_{OAWRS}$  was determined at OAWRS frequencies in the Lofoten region during the 2014 spawning season. In particular,  $TS_{OAWRS}$  was found to be -25.9 dB re 1 m (Fig.S3) by equating areal population density for nearly simultaneous OAWRS  $n_{A,OAWRS}(\rho_c)$  and RV Knorr 12 kHz echosounder  $n_{A,Knorr}(\rho_c)$  measurements in the Andenes region via  $TS_{OAWRS}(\rho_c) = SS_{OAWRS}(\rho_c) - 10 \log_{10}(n_{A,Knorr}(\rho_c))$  and averaging the result over 116 independent samples or resolution cells, following Makris et al. (2006a) and Makris et al. (2009a). This led to a  $TS_{OAWRS}$  error of 0.12 dB or 3 percent. The resulting OAWRS cod population density estimate was found to have a standard deviation of roughly 1-2 dB per pixel, which is within 1 dB of that obtained by resonance swimbladder modeling (Jain et al., 2013; Love, 1978) for the mean cod spawning length measured for the Lofoten region in 2014 (Fig.S4). This  $TS_{OAWRS}$  value of -25.9 dB re 1 m was used to estimate OAWRS cod areal population density throughout the Lofoten region for the 2014 spawning season.

### **S1.3 Consistency between OAWRS and line-transect vertical echosounder measurement**

Near Andenes Norway (Fig.S5), 12 kHz RV Knorr local vertical echosounder line-transect measurements were made simultaneously with OAWRS and showed consistent trends in cod population (Fig.S5). This consistency was also found in the Røst region where RV Knorr vertical echosounder measurements were made simultaneously with OAWRS measurements (Figs.S6A-D), and then roughly 5 hours (Figs.S6E-H) and roughly 24 hours after OAWRS imaging (Figs.S6I-L). Cod layers were consistently found at their preferred spawning depths near the 100 m contour where the transition layer between warm Atlantic waters and cold Arctic waters is typically found in the Lofoten region (Nuttall, 2012; Nakken, 2008) (Figs.S6A-L). Cod density distributions near Røst were temporally stable over a roughly one-month period (Fig.S7), as seen from the consistency between cod density distributions obtained by OAWRS on February 23, 2014 and by the annual line-transect vertical echosounder survey of March 17-31, 2014. The high cod density areas near Røst and general tapering trends radially away from Røst are clear and consistent in both OAWRS and vertical echosounder measurements.

We used data from the annual conventional line transect vertical acoustic echosounder survey of the cod spawning area (Korsbrekke, 1997) and associated stock assessment by the ICES Arctic Fisheries Working Group (ICES, 2014a) to evaluate the potential impact of other species on the OAWRS results. In 2014 the conventional line transect survey started at the end of the OAWRS Nordic Seas experiments on March 17, 2014 and continued until 31 March, covering the main cod concentration areas observed by OAWRS. The line transect survey carried out biological sampling with pelagic and demersal trawls to identify the species generating the acoustic backscatter. The estimated abundance was dominated by Northeast Arctic cod with minor quantities of saithe and haddock both of which were found outside the regions where OAWRS found large cod groups. The haddock appeared mostly in trawls towards the shelf-break and saithe were found to the southwest of the cod groups imaged by OAWRS near Røst. Coastal cod comprised a minor proportion of overall trawl catches and are not found to be part of typical Northeast Arctic cod spawning aggregations.

### **S1.4 OAWRS cod population density mosaic near Røst**

Shadowing by very shallow bathymetry or islands prevented the entire area around the underwater peninsula surrounding the Røst island from being imaged instantaneously by OAWRS from a single ship location (Fig.S8). Consequently, six instantaneous OAWRS images taken at locations around the Røst bathymetric feature at 10:40:49, 11:29:09, 12:13:19, 13:09:59, 14:04:59, and 15:07:29 UTC on February 23, 2014 were combined to generate the cod population density mosaic of Fig.1B. A running spatial averaging 1 km square window was applied to the raw OAWRS data of the Fig.1B mosaic to eliminate boundary discontinuities due to lack of temporal simultaneity of the six instantaneous images. Such smoothing was not necessary in Fig.1C since that image is not a mosaic.

### **S1.5 Critical boundary population density of cod spawning groups**

The critical population density defining the boundary of a gigantic cod shoal was consistently determined to be  $0.016 \text{ fish/m}^2$  by a number of independent methods including: (a) scaling the critical density consistently obtained experimentally with OAWRS for gigantic group formation in another oceanic fish species (Makris et al., 2009a) to account for body length ratios; (b) segmenting regions of high population density and gradient in OAWRS images; (c) segmenting regions of high population density and gradient in corresponding high-resolution line-transect

vertical echosounder measurements; (d) least squares estimation with decades of line-transect survey data of cod in the Northeast Arctic spawning ground.

The cod and herring spawning groups we study are horizontally extensive, stretching for tens of kilometers, and vertically thin, roughly one thousand times less than their horizontal extent. We find that the mean distance between nearest neighbors in the cod spawning groups we studied is 5 times greater in the horizontal than in the vertical, from high-resolution echo-sounding data. This makes the vertical separation component negligible when determining the magnitude of the separation vector between any two cod on average. The herring spawning group formation process and attainment of critical density has been shown to occur as herring leave the effectively 2-D horizontal surface of the seafloor. As with the cod, this leads to a mean horizontal separation much greater than the mean vertical separation for the herring groups (Makris et al., 2009a). Additionally, a number of studies have consistently found that the distance between fish in groups is proportional to fish body length (Pitcher & Partridge, 1979; Pavlov & Kasumyan, 2000; Misund, 1993). Given these facts, critical density for the horizontally extensive and vertically thin spawning groups of this study is expected to scale in proportion to fish body length squared. The separations between cod were determined from the positions of more than 150 cod individuals in the Andenes spawning group (Fig.S5). They were detected in a roughly 3 km transect through the spawning group at 02:40 UTC to 03:00 UTC on March 8, 2014 where the volume scattering coefficient ( $s_v$ ) was greater than -42 dB re 1 m<sup>-1</sup>. All detections were within the RV Johan Hjort 38 kHz echosounder's 6.8° main beam.

The boundary population density of a cod spawning group of 0.016 fish/m<sup>2</sup> is found to be the expected value of the critical density for cod spawning group formation based on thousands of independent and consistent OAWRS measurements of group formation in Atlantic herring (Makris et al., 2009a, 2009b, 2006b; Gong et al., 2014; Wang et al., 2016), which follow basic group behavioral principles (Misund, 1993). Since the separation between fish in groups is found to scale with body length (Pitcher & Partridge, 1979; Pavlov & Kasumyan, 2000; Misund, 1993) and the mean vertical separation between fish in the cod and herring groups studied is negligible compared to the mean horizontal separation, the critical density for cod group formation is found to be

$$c_{\text{cod}} = c_{\text{herring}} \left( \frac{L_{\text{herring}}}{L_{\text{cod}}} \right)^2 \quad (\text{S1})$$

by scaling the critical density for herring group formation (Makris et al., 2009a) by the squared ratio of herring to cod lengths where  $L_{\text{herring}}$  is the herring body length in the Fall 2006 Georges Bank spawning ground (Makris et al., 2006a), and  $L_{\text{cod}}$  is the cod body length measured in the Winter-Spring 2012-2014 Northeast Arctic cod spawning area (Fig.S4).

A simple contouring of population density at the critical density  $c_{\text{cod}}=0.016$  fish/m<sup>2</sup> in each wide-area OAWRS image, Figs.1B and 1C, led to segmentation of the high population density region that defined the two gigantic shoals shown. More than 90% of the detected cod fell within the closed boundary contour determined by the critical density  $c_{\text{cod}}=0.016$  fish/m<sup>2</sup> in these images (Figs.1B and 1C). The group boundary can also be detected from the spatial population density gradient, which is 5 times larger on the critical density contour than in the surrounding low density regions on average. The minimum cod population density detectable by OAWRS was roughly 0.005 fish/m<sup>2</sup>, where seafloor scattering mechanisms become a contaminant (Makris et al., 2009b; Jain et al., 2013). The population density standard deviation is roughly 1-2 dB (Makris et al., 2006a; Jagannathan et al., 2009). Raw OAWRS images are each comprised of hundreds of thousands of independent pixels since the OAWRS system has 15-m range resolution, and forms at least 64 independent horizontal beams, spanning ranges

of many tens of kilometers. The angular resolution of any beam away from endfire varies as  $\lambda/L \cos \theta$ , where  $\lambda$  is the acoustic wavelength,  $L$  is the receiver array aperture length and  $\theta$  is the horizontal angle from array broadside (Makris et al., 2006a; Jagannathan et al., 2009; Gong et al., 2010). In the raw OAWRS images corresponding to Figs.1B and 1C respectively, within the shoal boundary, for example, there are roughly 10,000 and 300,000 independent measurements or resolution cells, respectively and on the contour defining the shoal boundary, roughly 3,000 and 6,000 independent measurements respectively. So the OAWRS imagery alone provided thousands of independent samples to obtain the cod critical density. To reduce the standard deviation of Gaussian field fluctuations, it is conventional for 5 consecutive instantaneous raw OAWRS images to be averaged at each pixel with the additional averaging of two pixels in range to further reduce the standard deviation of Gaussian field fluctuations by  $1/\sqrt{10}$  (Makris, 1996; Tran et al., 2012; Makris et al., 2006a; Jagannathan et al., 2009). This was done for the OAWRS images presented Figs 1B and 1C. Some additional processing was done as described later for the Fig 1B mosaic.

Similar results were found with high-resolution vertical echosounder measurements by the RV Johan Hjort which was directed to cross the cod group found by OAWRS in Fig.1C. Again more than 90% of the cod detected with this echo-sounding data were within the region exceeding the  $0.016\text{fish}/\text{m}^2$  critical density which corresponded to the shoal boundary identified by OAWRS. The population density gradient at this critical density was two orders of magnitude larger than that found on average in the bordering low density regions by vertical echo-sounding. The RV Johan Hjort made more than 18,000 independent measurements of cod at and within the spawning group boundary shown in Fig.1C. It employed a 38 kHz high-resolution vertical echosounder system which has roughly 0.2-m range resolution, and forms a  $6.8^\circ$  main beam in the vertical direction.

The empirically derived critical density for cod group formation (Eq.S1) is also independently found to have the best least squares consistency with the annual spawning population time series and decades of line-transect survey data as shown in Fig.S9, under the assumption that summing the populations of spawning groups will well approximate the total annual spawning population each year. An unrealistically high value for group critical density will incorrectly exclude too much of the population. An unrealistically low value will incorrectly include background levels that have no cod information only noise. This consistency was found by searching for a threshold density  $n_{A,T}$  at which the  $i^{\text{th}}$  year's cod spawning population estimate  $S_{i,Q}(n_{A,T})$  best-matches  $i^{\text{th}}$  year's cod spawning population inferred by International Council for the Exploration of the Sea (ICES),  $S_{i,\text{ICES}}$ , over a 30-year period from 1984 to 2014 (Fig.S9), i.e.

$$\operatorname{argmin}_{n_{A,T}} \sum_{i=1}^M (S_{i,\text{ICES}} - S_{i,Q}(n_{A,T}))^2, \quad (\text{S2})$$

where  $M$  is the number of years. In Eq.S2, the  $i^{\text{th}}$  year's cod spawning population estimate  $S_{i,Q}(n_{A,T})$  is determined by multiplying the number of mean spawning groups in  $i^{\text{th}}$  year  $N_i(n_{A,T})$  by the mean spawning group size  $Q(n_{A,T})$  for given threshold density  $n_{A,T}$  as

$$S_{i,Q}(n_{A,T}) = N_i(n_{A,T})Q(n_{A,T}) = N_i(n_{A,T}) \frac{1}{M} \sum_{k=1}^M \frac{S_{k,\text{ICES}}}{N_k(n_{A,T})}. \quad (\text{S3})$$

The mean spawning group size  $\langle Q \rangle$  is then determined at the critical density for cod group formation  $c_{\text{cod}}$  by

$$\langle Q \rangle = Q(c_{\text{cod}}) = \sum_{k=1}^M \frac{S_{k,\text{ICES}}}{N_k(n_{A,T})} \Big|_{n_{A,T}=c_{\text{cod}}} . \quad (\text{S4})$$

## S1.6 Cod areal population density obtained by line-transect vertical echosounding

Cod areal population density was determined from RV Johan Hjort 38 kHz echosounder measurements near Andenes by

$$n_{A,\text{JH}} = \frac{1}{\sigma_{\text{bs}}} \int_{z_1}^{z_2} s_v dz, \quad (\text{S5})$$

where  $n_{A,\text{JH}}$  is the cod areal population density along RV Johan Hjort line transects,  $s_v$  is the calibrated volume backscattering coefficient in  $\text{m}^{-1}$  (MacLennan, Fernandes, & Dalen, 2002) at 38 kHz from RV Johan Hjort,  $z_1$  and  $z_2$  are the measured depth bounds of the groups vertical extent, which ranged roughly between 30 m and 100 m near Andenes,  $\sigma_{\text{bs}} = 10^{\text{TS}_{38 \text{ kHz}}/10}$  is the mean backscattering cross section of an individual fish at 38 kHz in units of  $\text{m}^2$ , and  $\text{TS}_{38 \text{ kHz}}$  is the empirical cod target strength at 38 kHz (MacLennan & Simmonds, 2013) corresponding to the mean cod length  $L$  measured in the region in 2014 (Fig.S4):

$$\text{TS}_{38 \text{ kHz}} = 20 \log_{10} L - 67.4 \quad (\text{S6})$$

Then, RV Knorr 12 kHz vertical echosounder line-transect measurements near Andenes were calibrated with the cod population density obtained from the RV Johan Hjort 38 kHz echosounder measurements in the same region. This was done by comparing the RV Knorr 12 kHz area backscattering strength ( $s_a$ ) measured at 03:22:45 UTC on March 8, 2014 with the cod areal population density measured from RV Johan Hjort at 03:15:00 UTC on March 8, 2014, such that peak areal population densities from the two research vessels match within 8 minutes in time and within 250 m in space. Negligible clipping occurred in the RV Knorr echosounder measurements used for this calibration.

## S2 Spawning group size distribution

### S2.1 Spawning group size distribution for Northeast Arctic cod

Cod spawning group size was obtained from the 30-year line-transect vertical echosounder data from 1984 to 2014 (Korsbrekke, 1997) by (a) spatially interpolating between line transects for each annual survey, (b) segmenting regions at and above the empirically determined group boundary threshold density of  $0.016 \text{ fish}/\text{m}^2$  to identify discrete spawning groups, and (c) integrating the cod population density over each segmented region. Each year's spawning group size distribution is normalized such that it integrates to the total ICES cod spawning population for that year (ICES, 2015a). The vertical echosounder measurements of cod archived in "Nautical Area Scattering Coefficients ( $\text{NASC}, s_A$ )" (MacLennan et al., 2002) were used to determine cod areal population densities  $n_A$  along the survey's line transects. This was done using the empirical length-dependent cod target strength  $\text{TS}_{38 \text{ kHz}}$  at 38 kHz (Eq.S6) determined from each year's mean cod length (Fig.S4) via  $n_A = s_A / (4\pi(1852)^2 \sigma_{\text{bs}})$ , where  $s_A$  is the nautical area scattering coefficients in  $\text{m}^2 \text{ nmi}^{-2}$ , and  $\sigma_{\text{bs}} = 10^{\text{TS}_{38 \text{ kHz}}/10}$  is the mean backscattering cross section of cod at 38 kHz in  $\text{m}^2$ . The mean cod length over 1985-2014 was used for the year 1984 where trawl catch data were not available. The annual Lofoten line-transect survey data (Korsbrekke, 1997) have been used to estimate annual Northeast Arctic cod spawning populations by ICES since 1985

(ICES, 2015a). Each year's mean spawning group size estimate has 30% error (Fig.3) which is dominated by uncertainties of each year's ICES inferred cod population (ICES, 2015a).

## **S2.2 Spawning group size for Georges Bank herring**

Mean spawning group size for Georges Bank herring was determined by averaging daily spawning group populations imaged by OAWRS over the 8-day peak herring spawning period from September 26 to October 3, 2006 on the northern flank of Georges Bank. The OAWRS herring population density images of fully developed large groups on each day were obtained from measured OAWRS intensities following the standard procedures described in Makris et al. (2006a), Jagannathan et al. (2009) and Gong et al. (2010). The resulting OAWRS herring density images have an error of roughly 1-2 dB in regions where group populations follow a stationary random process in space and time (Makris et al., 2006a; Jagannathan et al., 2009). The daily herring spawning populations were determined by integrating the OAWRS herring areal population densities at and above the measured group formation critical density of  $\rho_{crit}=0.2$  fish/m<sup>2</sup> for herring (Makris et al., 2009a). Analysis of historical herring line transect data (NEFSC, 2012) to estimate spawning group size was found to be impossible without unacceptable ambiguity due to severe spatial and temporal undersampling of spawning groups by the line transect method. This was due to the fact that the line-transect survey was primarily designed to survey all diffuse herring concentrations near the seafloor over the entire northern flank of Georges Bank with widely spaced transects over a two week period. The spawning groups, however, were found by OAWRS to form at specific times (evening) and locations (primarily central bank) over this same period (Makris et al., 2009a). As a result it was found that the predetermined line transects overwhelmingly missed spawning groups when both OAWRS and predetermined line-transect surveys were conducted simultaneously in the 2006 spawning season. Even when a predetermined line-transect passed through a spawning group in an annual survey, it did so only once in the group's small across-bank dimension, leaving the group's large along-bank dimension ambiguous. To our knowledge, all simultaneous measurements of spawning groups between OAWRS and conventional echo-sounding during 2006 occurred after the OAWRS vessel directed the conventional echo-sounding vessel to a given spawning group. The spawning groups observed by OAWRS did not coincide with the space-time trajectory of the planned line-transect survey, whose research vessel behaved as a Lagrangian particle in a spatially vast and temporally dynamic field of fish.

## **S3 Analysis of the total spawning population time series in the North Atlantic**

### **S3.1 Historic total spawning population time series in the North Atlantic**

Historic spawning stock abundance time series for Atlantic cod and Atlantic herring in four spawning grounds of the North Atlantic - US Northeast, Canada, North Sea, Norway - were reconstructed and investigated from before the industrial fishing age (earlier than the late 19th century) to present (Figs.7 and8).

Northeast Arctic cod: Spawning stock abundance time series of Northeast Arctic cod for 1946-2014 were obtained from reported stock numbers-at-age and proportion of mature-at-age data (ICES, 2015a), as

$$S_i = \sum_{j=0}^{a_{\max}} s_j^i \gamma_j^i, \quad (\text{S7})$$

where  $S_i$  is the spawning stock abundance in  $i^{\text{th}}$  year,  $a_{\max}$  is the maximum fish age,  $s_j^i$  is the stock numbers-at-age at age  $j$  in  $i^{\text{th}}$  year, and  $\gamma_j^i$  is the proportion of mature-at-age for age  $j$  in  $i^{\text{th}}$  year. For 1876-1956, cod spawning stock biomass time series were derived from Catch-Per-Unit-Effort (CPUE) estimates obtained using official Norwegian annual cod catch and fishing effort data in Godø (2003). Spawning stock abundance of Northeast Arctic cod in 1876-1945 was then estimated by dividing biomass time series by a representative weight per cod value of 3.8 kg/fish. This 3.8 kg/fish weight per cod value was obtained in a least squares sense between biomass time series divided by a weight per cod and abundance time series in 1946-2013 from

$$\operatorname{argmin}_w \sum_{i=1}^M \left( S_i - \frac{\text{SSB}_i}{w} \right)^2, \quad (\text{S8})$$

where  $w$  is the weight per fish,  $M$  is the number of years,  $S_i$  is the spawning stock abundance in  $i^{\text{th}}$  year, and  $\text{SSB}_i$  is the spawning stock biomass in  $i^{\text{th}}$  year. The spawning stock abundance in Lofoten spawning grounds where OAWRS imaging and annual line-transect acoustic survey took place was derived by multiplying the spawning stock abundance of entire Northeast Arctic cod population by a factor of 2/3 (Brander, 2005).

US Gulf of Maine cod: Spawning stock abundance time series of US Gulf of Maine cod for 1982-2013 were obtained from reported stock numbers-at-age and proportion of mature-at-age data (NOAA, 2014) via Eq.S7. For 1963-1994, cod spawning stock biomass time series of US Gulf of Maine cod was available from NOAA (1996). Spawning stock abundance of US Gulf of Maine cod in 1963-1981 was then estimated by dividing biomass time series by a representative weight per cod value of 1.75 kg/fish. This 1.75 kg/fish weight per cod value was obtained by minimizing the least square difference between biomass time series divided by a weight per cod and abundance time series in 1982-1994 (Eq.S8). Historic spawning stock abundance time series of US Gulf of Maine cod in 1891-1914 and 1931-1965 were estimated by determining a scale factor for CPUE time series for US Georges Bank cod in 1891-1914 and 1931-1965 (Serchuk & Wigley, 1992) to match US Gulf of Maine spawning stock abundance in 1963-1965, where both time series were available, from

$$\operatorname{argmin}_\lambda \sum_{i=1}^M (\lambda I_i - S_i)^2, \quad (\text{S9})$$

where  $\lambda$  is the scale factor,  $M$  is the number of years,  $I_i$  is the quantity to be scaled such as CPUE to match  $S_i$  in  $i^{\text{th}}$  year, and  $S_i$  is the spawning stock abundance in  $i^{\text{th}}$  year. The CPUE estimates for Gulf of Maine cod in 1891-1914 and 1931-1965 were assumed to have the same temporal trends as those for Georges Bank cod reported in Serchuk and Wigley (1992).

Canada Northern cod (Atlantic cod in the statistical area 2J3KL): Spawning stock biomass time series of Canadian Northern cod for 1983-2012 and 1962-1982 were obtained from DFO (2013) and DFO (1998a), respectively. Spawning stock abundance of Canadian Northern cod in 1962-1993 and 2010-2012 was then estimated by dividing spawning stock biomass by mean weight per cod value of 2.4 kg/fish obtained for 2009 (DFO, 2010). Spawning stock abundance of Canadian Northern cod in 1994-2009 was estimated by dividing spawning stock biomass by each year's mean weight per cod values varying roughly between 0.5 and 3.1 kg/fish (DFO, 2010, 2009, 2008, 2006, 2005, 2004, 2003, 2001, 2000, 1999, 1998b, 1996, 1995). Each years' mean weight per cod was found from number of samples caught-at-age, proportion of mature-at-age, and

mean sample weight-at-age (DFO, 2010, 2009, 2008, 2006, 2005, 2004, 2003, 2001, 2000, 1999, 1998b, 1996, 1995). The averaged weight per cod of 1995 and 1997 was used for the year 1996 where catch data were not available. Historic spawning stock abundance time series of Canadian Northern cod in 1550-1800 were estimated by determining a scale factor for cod stock biomass time series of the entire Eastern Canadian waters in 1550-2004 (Rose, 2004) to match Northern cod spawning stock abundance in 1962 (DFO, 1998a) via Eq.S9 assuming a steady-state in the regional distribution of historic cod populations in the Eastern Canadian waters.

North Sea cod: Spawning stock abundance time series of North Sea cod for 1963-2014 were obtained from reported stock numbers-at-age and proportion of mature-at-age data (ICES, 2014a) via Eq.S7. For 1910-1960, cod spawning stock biomass time series was available from Daan, Heessen, and Pope (1994). Spawning stock abundance of North Sea cod in 1910-1960 was then estimated by dividing biomass time series by a representative weight per cod value of 3.1 kg/fish. This 3.1 kg/fish weight per cod value was obtained by minimizing the least square difference between biomass time series divided by a weight per cod and abundance time series in 1963-2014 (Eq.S8). Historic cod spawning stock abundance in 1889-1893 was obtained by determining a scale factor for the mean spawning stock abundance in 2003-2007 as the ratio of Landing Per Unit fishing Power (LPUP) in 1889-1893 to those in 2003-2007 (Thurstan, Brockington, & Roberts, 2010).

Norwegian Spring-spawning herring: Spawning stock abundance times series of Norwegian Spring-spawning herring in 1988-2014 were obtained from reported stock numbers-at-age and proportion of mature-at-age data (ICES, 2014b) via Eq.S7. For 1907-1998, herring spawning stock biomass time series was available from Toresen and Østvedt (2000). Spawning stock abundance of Norwegian Spring-spawning herring in 1907-1987 was then estimated by dividing biomass time series by a representative weight per herring value of 0.28 kg/fish. This 0.28 kg/fish weight per herring value was obtained by minimizing the least square difference between biomass time series divided by a weight per herring and abundance time series in 1988-2014 (Eq.S8).

North Sea herring: Spawning stock abundance time series of North Sea herring in 1947-2014 were obtained from reported stock numbers-at-age and proportion of mature-at-age data (ICES, 2015b) via Eq.S7. Historic herring spawning abundance time series in 1600-1800 was obtained by determining a scale factor for CPUE time series of North Sea herring in 1600-1966 (ICES, 2008) to match North Sea herring spawning stock abundance in 1947-1966 via Eq.S9, where both time series were available.

US Georges Bank herring: Spawning stock biomass time series of Gulf of MaineGB (GoM-GB) herring population complex in 1965-2014 were obtained from NOAA (2015). For 1880-1964, spawning stock biomass of GoM-GB herring complex was estimated by employing a surplus production model with fisheries data in 1880-2007 in the Gulf of Maine (Klein, 2008) via Eq.S10. The herring fisheries data in 1880-2007 obtained from Klein (2008) was scaled to represent entire GoM-GB fisheries catch by an inverse of  $(1 - \text{mean ratio of Georges Bank herring stock to entire GoM-GB herring complex (NEFSC, 2012)})$ , and then used as an input to the surplus production model. Since the surplus production model outputs the total stock biomass, the mean ratio of the spawning stock biomass to total stock biomass as well as the mean ratio of Georges Bank herring stock to entire GoM-GB herring complex are multiplied to the output of the model to obtain spawning stock biomass of Georges Bank herring. The 3-year running averages of ratio of Georges Bank herring stock to entire GoM-GB herring complex was used for Fig.6C (NEFSC, 2012). Herring spawning stock abundance was estimated by dividing spawning stock biomass by a representative weight per herring of 0.1 kg/fish (NEFSC, 2012).

Canada Southwest (SW) Nova Scotia herring (SW Nova Scotia/Bay of Fundy Atlantic herring in the statistical area 4VWX): Spawning stock biomass of SW Nova Scotia and Bay of Fundy herring in 4VWX statistical area in 1965-2006 was obtained from Fisheries and Canada (2006). For 1880-2007, historic herring spawning stock biomass of SW Nova Scotia and Bay of Fundy herring was estimated by employing a surplus production model with fisheries data in 1880-2007 in Bay of Fundy (Klein, 2008) via Eq.S10. The herring fisheries data in 1880-2007 obtained from Klein (2008) was used as an input to the surplus production model. Since the surplus production model outputs the total stock biomass, the ratio of spawning stock biomass to total stock biomass was multiplied to the output of the model to obtain spawning stock biomass of SW Nova Scotia/Bay of Fundy herring. Herring spawning stock abundance was estimated by dividing spawning stock biomass by a representative weight per herring of 0.1 kg/fish.

### S3.2 Surplus production model for Atlantic herring populations

A surplus production model was employed to estimate historic herring spawning stock abundance in Georges Bank and Southwest Nova Scotia/Bay of Fundy from the late 19th century to present. A similar approach appears in Rose (2004) for Atlantic cod biomass in the entire Eastern Canadian waters. The employed surplus production model is based on an equation (Rose, 2004):

$$B_y = B_{y-1} + r_b \frac{B_{y-1}}{aK + B_{y-1}} B_{y-1} \left[ 1 - \frac{B_{y-1}}{K} \right] - C_{y-1}, \quad (\text{S10})$$

where  $B_y$  is the total stock biomass in year  $y$ ,  $r_b$  is the intrinsic rate of population growth expected without the depensation effect,  $K$  is the carrying capacity of the ecosystem or the initial biomass,  $a$  is the depensation parameter, and  $C_y$  is the fisheries catch data in year  $y$ . The depensation parameter  $a$  is set to be zero for  $B_y > K/2$  and given a value of 0.06 (Rose, 2004) for  $B_y \leq K/2$ . Historic stock biomass  $K$  before industrial fishing began and the parameter  $r_b$  were determined by searching for the values at which available stock biomass data time series best-match the surplus production model estimate time series such that the percentage error in surplus production model fit is minimized:

$$\operatorname{argmin}_{r_b, K} \sqrt{\frac{\sum_{i=1}^M (B_{i,\text{data}} - B_{i,SP}(r_b, K))^2}{\sum_{i=1}^M B_{i,\text{data}}^2}} \times 100, \quad (\text{S11})$$

where  $r_b$  is the intrinsic rate of population growth expected without the depensation effect,  $K$  is the carrying capacity of the ecosystem or the stock biomass before industrial fishing began,  $M$  is the number of years,  $B_{i,\text{data}}$  is the available stock biomass data in  $i^{\text{th}}$  year, and  $B_{i,SP}$  is the surplus production model stock biomass estimate in  $i^{\text{th}}$  year. The ranges of historic spawning stock abundance for Georges Bank herring and SW Nova Scotia/Bay of Fundy herring in Fig.6C were determined at 30% error in surplus production model fit to data.

### S3.3 Time to return to pre-industrial levels after a decline to within a standard deviation of the mean group size

The time ( $T_{\text{return}}$ ) required for a total spawning population time series ( $S$ ) that has declined to within a standard deviation of the mean spawning group size or quantum ( $A = q + \sigma$ ) to return to its pre-industrial level ( $B$ ) is determined via the following procedure, where  $S_i$  is the total spawning population in the  $i^{\text{th}}$  year,  $i = 1, \dots, N$ ,  $N$  is the total number of years, and  $\Delta T$  is the time interval between  $S_i$  and  $S_{i+1}$ :

1. Define an index  $D = \{i | (S_i - A)(S_{i+1} - A) < 0\}$  such that the total spawning population time series crosses the quantum level  $A$  at the years in  $S$ .
2. Find the earliest year at which  $S$  declines below  $A$ ,  $i_D = \min(D)$ .
3. Define an index  $P = \{i | (S_i - B)(S_{i+1} - B) < 0 \text{ and } i > i_D\}$  such that  $S$  crosses pre-industrial level  $B$  at the years in  $S$ .
4. Find the earliest year at which  $S$  returns to  $B$ ,  $i_P = \min(P)$  when  $n(P) > 0$ . If the total spawning population does not return to pre-industrial level, the largest year index  $N$  is used for  $i_P$ , i.e.  $i_P = N$  when  $n(P) = 0$ .
5.  $T_{\text{return}}$  is determined to be  $(i_P - i_D)\Delta T$  when  $n(P) > 0$  and  $T_{\text{return}}$  is greater than  $(i_P - i_D)\Delta T$  when  $n(P) = 0$ .

By this analytic algorithm, it is found that some spawning populations have returned to pre-industrial levels after declining to within a standard deviation of the mean spawning group size measured from a population at pre-industrial levels, or quantum. In particular, it took Northeast Arctic cod 47 years to return to pre-industrial level after declining to within a standard deviation of a cod quantum. The total spawning populations of Gulf of Maine cod, Canadian Northern cod and North Sea cod declined to within a standard deviation from a cod quantum 67, 25 and 29 years ago respectively, and have not yet returned to pre-industrial levels. For Norwegian herring and Georges Bank herring, it took 20 and 13 years respectively to return to pre-industrial levels after a population decline to within a standard deviation from a herring quantum.

### S3.4 Population growth rate

The population growth rate  $R_i$  in the  $i^{\text{th}}$  year is defined through a logarithmic function as (Rockwood, 2015; Sibly & Hone, 2002):

$$R_i = \frac{10 \log_{10} \frac{S_{i+1}}{S_i}}{\Delta T}, \quad (\text{S12})$$

where  $S_i$  is the total spawning population in  $i^{\text{th}}$  year,  $\Delta T$  is the time between  $S_i$  and  $S_{i+1}$ ,  $i = 1, \dots, N - 1$ , and  $N$  is the total number of years. The population growth rates obtained each year from 1920 to 2014 are shown as a function of total spawning population for each population we investigated (Figs.S10 and S11).

## References

- Brander, K. (2005). Spawning and life history information for north atlantic cod stocks. *ICES cooperative research report*.
- Chen, T., Ratilal, P., & Makris, N. C. (2005). Mean and variance of the forward field propagated through three-dimensional random internal waves in a continental-shelf waveguide. *The Journal of the Acoustical Society of America*, 118(6), 3560–3574.
- Collins, M. D. (1993). A split-step padé solution for the parabolic equation method. *The Journal of the Acoustical Society of America*, 93(4), 1736–1742.
- Daan, N., Heessen, H. J., & Pope, J. G. (1994). Changes in the north sea cod stock during the twentieth century. In *Ices marine science symposia* (Vol. 198, pp. 229–243).
- DFO. (1995). *Canadian government 1995 stock assessment report on northern cod*. [http://www.dfo-mpo.gc.ca/csas-sccs/Publications/ResDocs-DocRech/1995/1995\\_034\\_e.pdf](http://www.dfo-mpo.gc.ca/csas-sccs/Publications/ResDocs-DocRech/1995/1995_034_e.pdf).
- DFO. (1996). *Canadian government 1996 stock assessment report on northern cod*. [http://www.dfo-mpo.gc.ca/csas-sccs/Publications/ResDocs-DocRech/1996/1996\\_080\\_e.pdf](http://www.dfo-mpo.gc.ca/csas-sccs/Publications/ResDocs-DocRech/1996/1996_080_e.pdf).

- DFO. (1998a). *Canadian government 1998 report on northern cod*. <http://archive.nafo.int/open/sc/1998/scr-98-046.pdf>.
- DFO. (1998b). *Canadian government 1998 stock assessment report on northern cod*. [http://www.dfo-mpo.gc.ca/csas-sccs/Publications/ResDocs-DocRech/1998/98\\_015\\_e.pdf](http://www.dfo-mpo.gc.ca/csas-sccs/Publications/ResDocs-DocRech/1998/98_015_e.pdf).
- DFO. (1999). *Canadian government 1999 stock assessment report on northern cod*. [http://www.dfo-mpo.gc.ca/csas-sccs/Publications/ResDocs-DocRech/1999/pdf/99\\_042e2.pdf](http://www.dfo-mpo.gc.ca/csas-sccs/Publications/ResDocs-DocRech/1999/pdf/99_042e2.pdf).
- DFO. (2000). *Canadian government 2000 stock assessment report on northern cod*. [http://www.dfo-mpo.gc.ca/csas-sccs/Publications/ResDocs-DocRech/2000/PDF/2000\\_063e.pdf](http://www.dfo-mpo.gc.ca/csas-sccs/Publications/ResDocs-DocRech/2000/PDF/2000_063e.pdf).
- DFO. (2001). *Canadian government 2001 stock assessment report on northern cod*. [http://www.dfo-mpo.gc.ca/csas-sccs/Publications/ResDocs-DocRech/2001/RES2001\\_044e.pdf](http://www.dfo-mpo.gc.ca/csas-sccs/Publications/ResDocs-DocRech/2001/RES2001_044e.pdf).
- DFO. (2003). *Canadian government 2003 stock assessment report on northern cod*. [http://www.dfo-mpo.gc.ca/csas-sccs/Publications/ResDocs-DocRech/2003/RES2003\\_023\\_e.pdf](http://www.dfo-mpo.gc.ca/csas-sccs/Publications/ResDocs-DocRech/2003/RES2003_023_e.pdf).
- DFO. (2004). *Canadian government 2004 stock assessment report on northern cod*. [http://www.dfo-mpo.gc.ca/csas-sccs/Publications/ResDocs-DocRech/2004/RES2004\\_023\\_e.pdf](http://www.dfo-mpo.gc.ca/csas-sccs/Publications/ResDocs-DocRech/2004/RES2004_023_e.pdf).
- DFO. (2005). *Canadian government 2005 stock assessment report on northern cod*. [http://www.dfo-mpo.gc.ca/csas-sccs/Publications/ResDocs-DocRech/2005/RES2005\\_018\\_e.pdf](http://www.dfo-mpo.gc.ca/csas-sccs/Publications/ResDocs-DocRech/2005/RES2005_018_e.pdf).
- DFO. (2006). *Canadian government 2006 stock assessment report on northern cod*. [http://www.dfo-mpo.gc.ca/csas-sccs/Publications/ResDocs-DocRech/2006/RES2006\\_043\\_e.pdf](http://www.dfo-mpo.gc.ca/csas-sccs/Publications/ResDocs-DocRech/2006/RES2006_043_e.pdf).
- DFO. (2008). *Canadian government 2008 stock assessment report on northern cod*. [http://www.dfo-mpo.gc.ca/csas-sccs/Publications/ResDocs-DocRech/2008/2008\\_086\\_e.pdf](http://www.dfo-mpo.gc.ca/csas-sccs/Publications/ResDocs-DocRech/2008/2008_086_e.pdf).
- DFO. (2009). *Canadian government 2009 stock assessment report on northern cod*. <http://waves-vagues.dfo-mpo.gc.ca/Library/338689.pdf>.
- DFO. (2010). *Canadian government 2010 stock assessment report on northern cod*. <http://waves-vagues.dfo-mpo.gc.ca/Library/342532.pdf>.
- DFO. (2013). *Canadian government 2013 report on northern cod*. [http://www.dfo-mpo.gc.ca/csas-sccs/Publications/SAR-AS/2013/2013\\_014-eng.pdf](http://www.dfo-mpo.gc.ca/csas-sccs/Publications/SAR-AS/2013/2013_014-eng.pdf).
- Fisheries, & Canada, O. (2006). *Canadian government 2006 report on 4vwx herring*. [http://www.dfo-mpo.gc.ca/csas/Csas/status/2006/SAR-AS2006\\_031\\_E.pdf](http://www.dfo-mpo.gc.ca/csas/Csas/status/2006/SAR-AS2006_031_E.pdf).
- Godø, O. R. (2003). Fluctuation in stock properties of north-east arctic cod related to long-term environmental changes. *Fish and Fisheries*, 4(2), 121–137.
- Gong, Z., Andrews, M., Jagannathan, S., Patel, R., Jech, J. M., Makris, N. C., & Ratilal, P. (2010). Low-frequency target strength and abundance of shoaling atlantic herring (*clupea harengus*) in the gulf of maine during the ocean acoustic waveguide remote sensing 2006 experiment. *The Journal of the Acoustical Society of America*, 127(1), 104–123.
- Gong, Z., Jain, A. D., Tran, D., Yi, D. H., Wu, F., Zorn, A., ... Makris, N. C. (2014). Ecosystem scale acoustic sensing reveals humpback whale behavior synchronous with herring spawning processes and re-evaluation finds no effect of sonar on humpback song occurrence in the gulf of maine in fall 2006. *PloS one*, 9(10), e104733.
- ICES. (2008). *Ices 2008 workshop report*. <http://www.ices.dk/sites/pub/Publication%20Reports/Expert%20Group%20Report/rmc/2008/WKHIST/WKHIST%20Executive%20Summary.pdf>.
- ICES. (2014a). *Ices 2014 report on north sea cod*. <http://www.ices.dk/sites/pub/Publication%20Reports/Expert%20Group%20Report/acom/2014/WGNSSK/>

- 01%20WGNSSK%20report%202014.pdf.
- ICES. (2014b). *Ices 2014 report on norwegian spring-spawning herring*. <http://www.ices.dk/sites/pub/Publication%20Reports/Expert%20Group%20Report/acom/2014/WGWIDE/01%20WGWIDE%20report%202014.pdf>.
- ICES. (2015a). *Ices 2015 afgw report*. <http://www.ices.dk/sites/pub/Publication%20Reports/Expert%20Group%20Report/acom/2015/AFWG/01%20AFWG%20Report%202015.pdf>.
- ICES. (2015b). *Ices 2015 report on north sea herring*. <http://www.ices.dk/sites/pub/Publication%20Reports/Expert%20Group%20Report/acom/2015/HAWG/01%20HAWG%20Report%202015.pdf>.
- Jagannathan, S., Bertsatos, I., Symonds, D., Chen, T., Nia, H. T., Jain, A. D., ... others (2009). Ocean acoustic waveguide remote sensing (oawrs) of marine ecosystems. *Marine Ecology Progress Series*, 395, 137–160.
- Jain, A. D., Ignisca, A., Yi, D. H., Ratilal, P., & Makris, N. C. (2013). Feasibility of ocean acoustic waveguide remote sensing (oawrs) of atlantic cod with seafloor scattering limitations. *Remote Sensing*, 6(1), 180–208.
- Klein, E. (2008). *A new perspective: Atlantic herring (clupea harengus) as a case study for time series analysis and historical data*. University of New Hampshire.
- Korsbrekke, K. (1997). Norwegian acoustic survey of north east arctic cod on the spawning grounds off lofoten. ICES Document CM 1997/Y:18.
- Love, R. H. (1978). Resonant acoustic scattering by swimbladder-bearing fish. *The Journal of the Acoustical Society of America*, 64(2), 571–580.
- MacLennan, D. N., Fernandes, P. G., & Dalen, J. (2002). A consistent approach to definitions and symbols in fisheries acoustics. *ICES Journal of Marine Science*, 59(2), 365–369.
- MacLennan, D. N., & Simmonds, E. J. (2013). *Fisheries acoustics* (Vol. 5). Springer Science & Business Media.
- Makris, N. C. (1996). The effect of saturated transmission scintillation on ocean acoustic intensity measurements. *The Journal of the Acoustical Society of America*, 100(2), 769–783.
- Makris, N. C., Ratilal, P., Jagannathan, S., Gong, Z., Andrews, M., Bertsatos, I., ... Jech, J. M. (2009a). Critical population density triggers rapid formation of vast oceanic fish shoals (with supporting online material). *Science*, 323(5922), 1734–1737.
- Makris, N. C., Ratilal, P., Jagannathan, S., Gong, Z., Andrews, M., Bertsatos, I., ... Jech, J. M. (2009b). *Supporting online material for critical population density triggers rapid formation of vast oceanic fish shoals (2009, science)*. [www.sciencemag.org/cgi/content/full/323/5922/1734/DC1](http://www.sciencemag.org/cgi/content/full/323/5922/1734/DC1).
- Makris, N. C., Ratilal, P., Symonds, D. T., Jagannathan, S., Lee, S., & Nero, R. W. (2006a). Fish population and behavior revealed by instantaneous continental shelf-scale imaging (with supporting online material). *Science*, 311(5761), 660–663.
- Makris, N. C., Ratilal, P., Symonds, D. T., Jagannathan, S., Lee, S., & Nero, R. W. (2006b). *Supporting online material for fish population and behavior revealed by instantaneous continental shelf-scale imaging (2006, science)*. [www.sciencemag.org/cgi/content/full/311/5761/660/DC1](http://www.sciencemag.org/cgi/content/full/311/5761/660/DC1).
- Misund, O. A. (1993). Dynamics of moving masses: variability in packing density, shape, and size among herring, sprat, and saithe schools. *ICES Journal of Marine Science*, 50(2), 145–160.
- Nakken, O. (2008). *Norwegian spring-spawning herring & northeast arctic cod: 100 years of research management*. Tapir Academic Press.
- NEFSC. (2012). *54th northeast regional stock assessment workshop (54th saw) assessment report*. <http://www.nefsc.noaa.gov/publications/crd/crd1218/>. NOAA National Ma-

- rine Fisheries Service, Northeast Fisheries Science Center, 166 Water Street, Woods Hole, MA 02543.
- NOAA. (1996). *Noaa 1996 report on us northeast cod*. <http://nefsc.noaa.gov/publications/crd/pdfs/crd9605c.pdf>.
- NOAA. (2014). *Noaa 2014 report on gulf of maine cod*. [http://www.nefsc.noaa.gov/saw/cod/pdfs/GoM\\_cod\\_2014\\_update\\_20140822.pdf](http://www.nefsc.noaa.gov/saw/cod/pdfs/GoM_cod_2014_update_20140822.pdf).
- NOAA. (2015). *Noaa 2015 report on us herring*. <https://www.nefsc.noaa.gov/nefsc/publications/crd/crd1516/crd1516.pdf>.
- Nuttall, M. (2012). *Encyclopedia of the arctic*. Routledge.
- Pavlov, D., & Kasumyan, A. (2000). Patterns and mechanisms of schooling behavior in fish: a review. *Journal of Ichthyology*, *40*(2), S163.
- Pitcher, T., & Partridge, B. (1979). Fish school density and volume. *Marine Biology*, *54*(4), 383–394.
- Rockwood, L. L. (2015). *Introduction to population ecology*. John Wiley & Sons.
- Rose, G. (2004). Reconciling overfishing and climate change with stock dynamics of atlantic cod (*gadus morhua*) over 500 years. *Canadian Journal of Fisheries and Aquatic Sciences*, *61*(9), 1553–1557.
- Serchuk, F. M., & Wigley, S. E. (1992). Assessment and management of the georges bank cod fishery: an historical review and evaluation. *J. Northw. Atl. Fish. Sci.*, *13*, 25–52.
- Sibly, R. M., & Hone, J. (2002). Population growth rate and its determinants: an overview. *Philosophical Transactions of the Royal Society of London B: Biological Sciences*, *357*(1425), 1153–1170.
- Thurstan, R. H., Brockington, S., & Roberts, C. M. (2010). The effects of 118 years of industrial fishing on uk bottom trawl fisheries. *Nature communications*, *1*, 15.
- Toresen, R., & Østvedt, O. J. (2000). Variation in abundance of norwegian spring-spawning herring (*clupea harengus*, clupeidae) throughout the 20th century and the influence of climatic fluctuations. *Fish and Fisheries*, *1*(3), 231–256.
- Tran, D., Andrews, M., & Ratilal, P. (2012). Probability distribution for energy of saturated broadband ocean acoustic transmission: Results from gulf of maine 2006 experiment. *The Journal of the Acoustical Society of America*, *132*(6), 3659–3672.
- Wang, D., Garcia, H., Huang, W., Tran, D. D., Jain, A. D., Yi, D. H., . . . others (2016). Vast assembly of vocal marine mammals from diverse species on fish spawning ground. *Nature*, *531*(7594), 366.

## Supplementary Figures

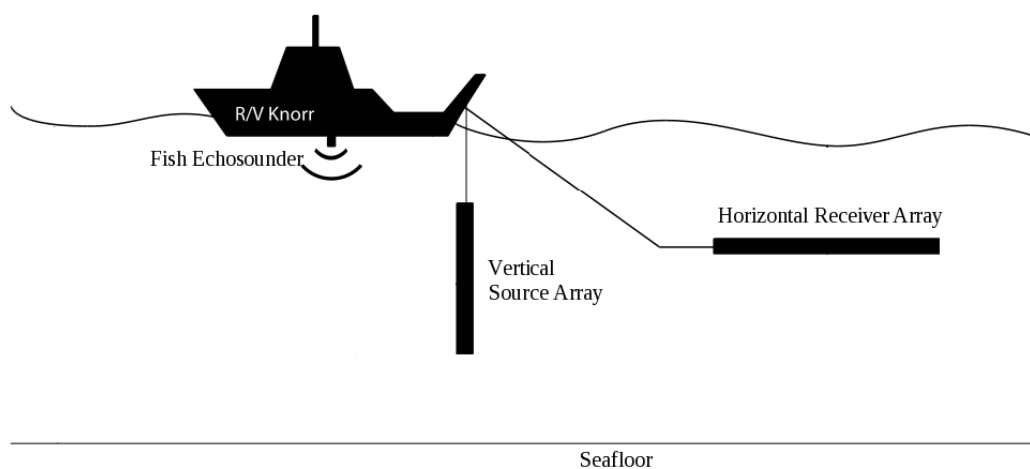


Figure S1: OAWRS system used for cod measurements during the Nordic Seas 2014 Experiment. Effectively monostatic OAWRS system where source and receiver arrays were towed from the same research vessel RV Knorr. The OAWRS source was developed under the National Science Foundation and Sloan Foundation MRI program for wide-area sensing of marine life, and the ONR Five Octave Research Array (FORA) was used as the OAWRS receiver.

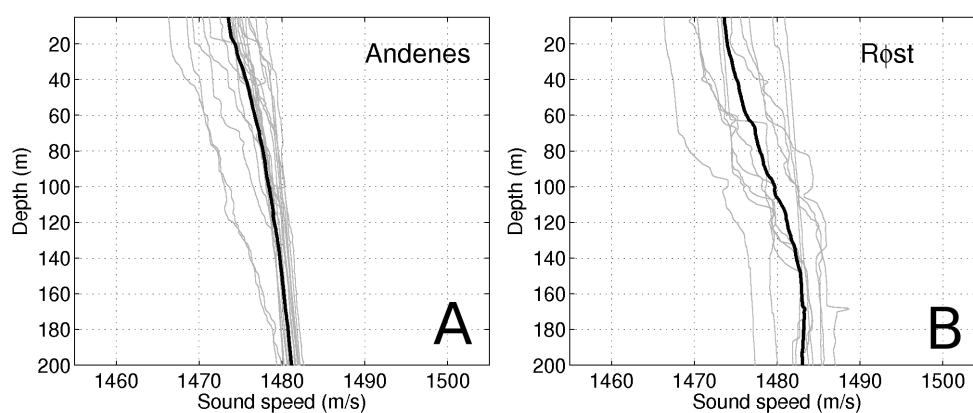


Figure S2: Measured vertical sound speed profiles via XBT and CTD during Nordic Seas 2014 Experiment near Andenes (A) and Røst (B).

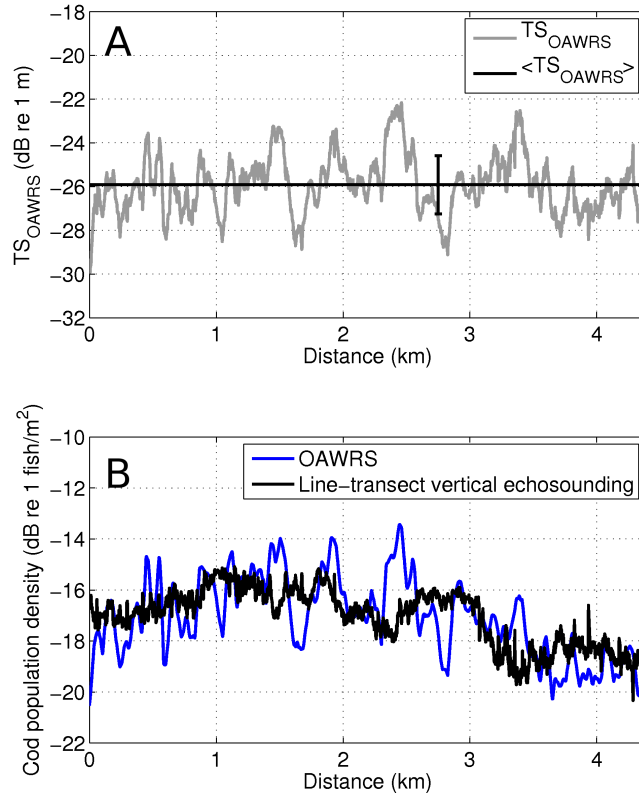


Figure S3: Expected cod target strength  $\langle TS_{OAWRS} \rangle$  at OAWRS frequencies was determined (A) by matching the cod areal population density obtained from the 12 kHz RV Knorr vertical echosounder measurements at 01:51:00-02:20:24 UTC and that from the OAWRS image at 01:26:49 UTC on March 8, 2014 for corresponding locations along the RV Knorr's line transect (B).

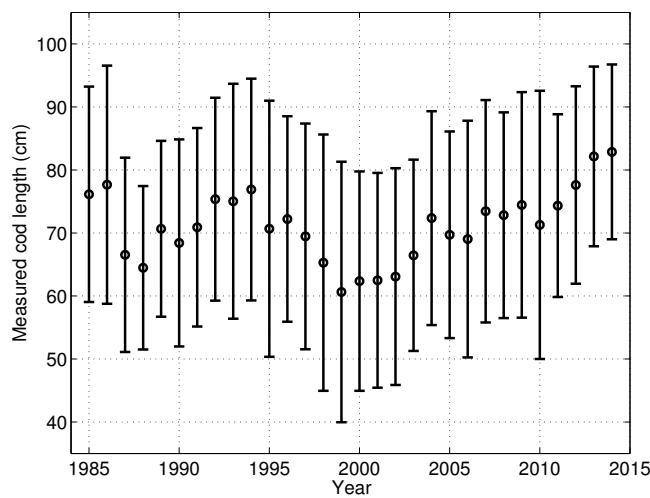


Figure S4: Time series of mean (circles) and standard deviation (vertical lines) of Atlantic cod length measured from annual trawl survey in the Lofoten spawning ground of the Northeast Arctic population from 1985-2014.

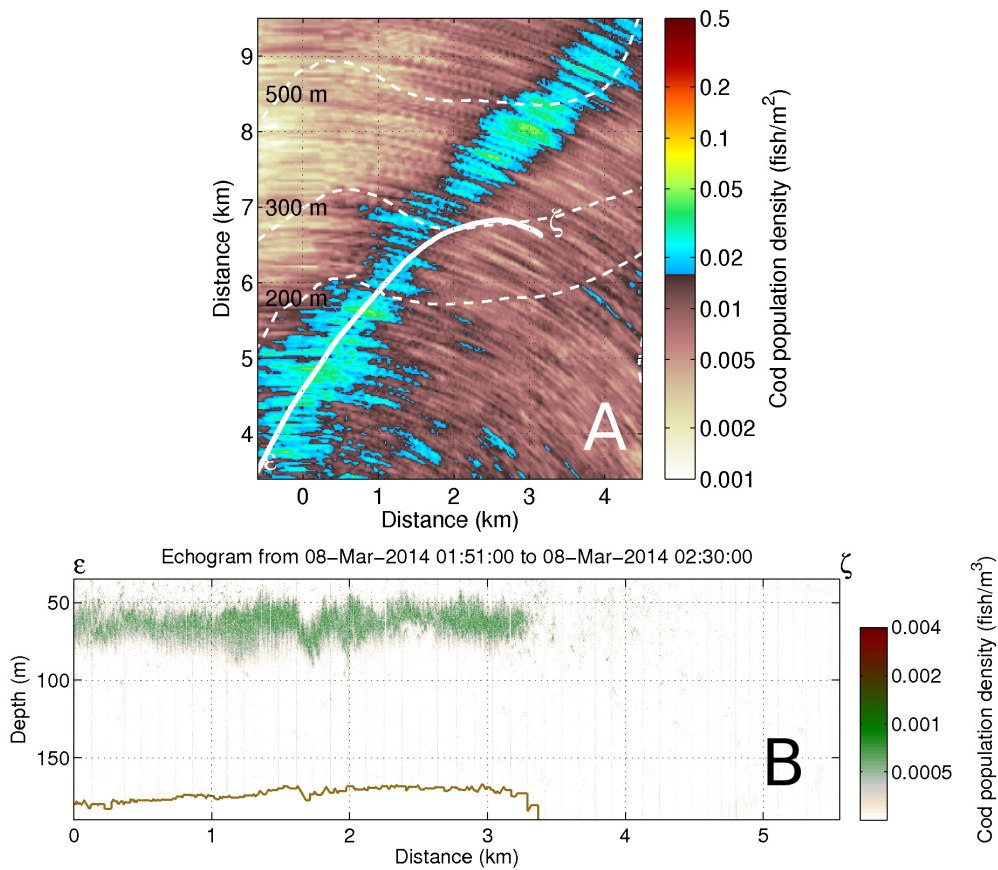


Figure S5: Correspondence between (A) an instantaneous OAWRS cod population density image and (B) 12 kHz RV Knorr vertical echosounder line-transect measurements near Andenes. The OAWRS cod population density image (A) was obtained near Andenes at 01:26:49 UTC on March 8, 2014. The 12 kHz RV Knorr vertical echosounder line-transect measurements (B) were made from 01:51:00 to 02:20:24 UTC on March 8, 2014. The white line transect in (A) passing through the group imaged by OAWRS is the RV Knorr track with corresponding vertical echosounder data shown in (B).

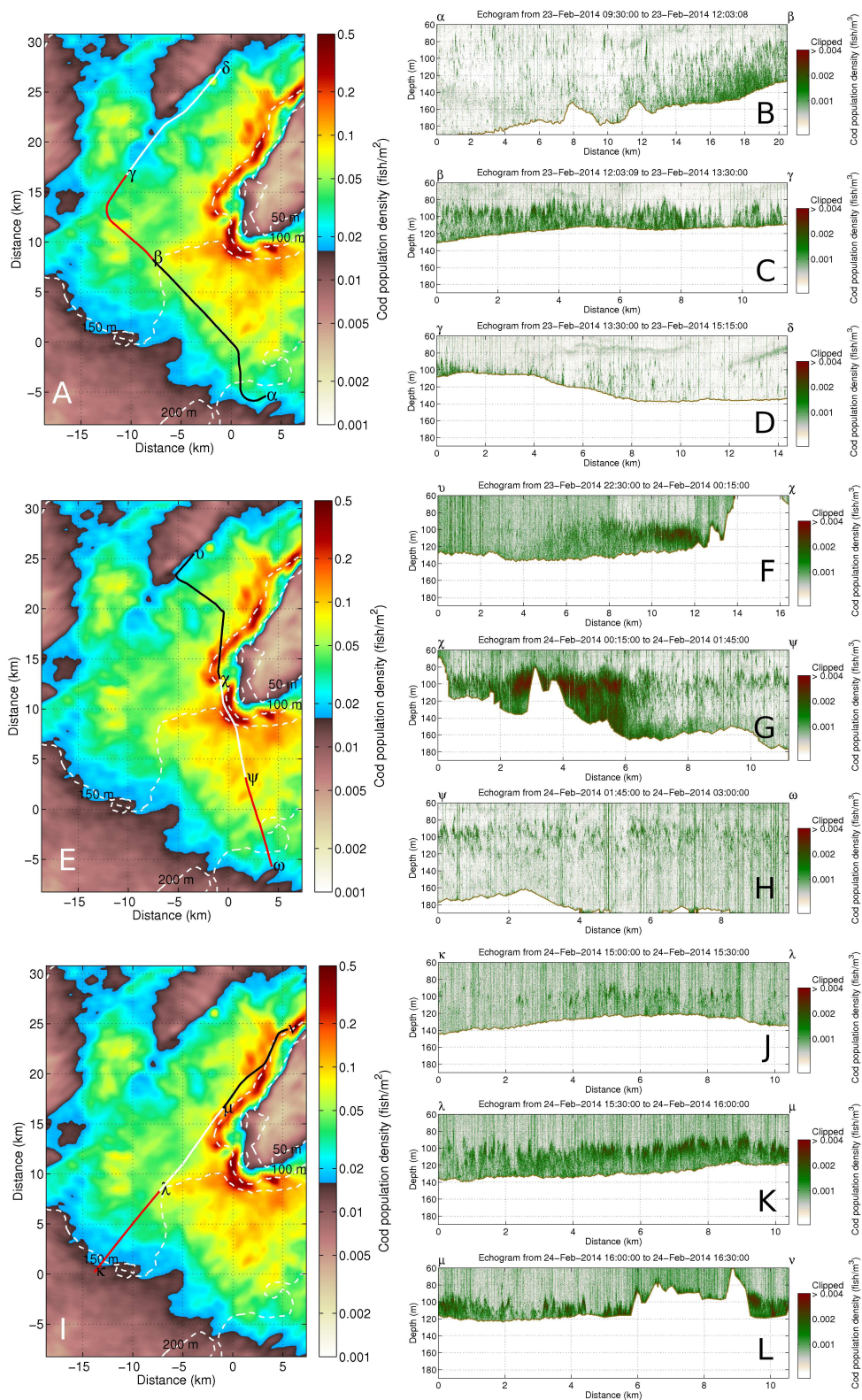


Figure S6: Correspondence between OAWRS and RV Knorr line-transect vertical echosounder measurements of cod near Røst. (A-D) Simultaneous correspondence between OAWRS imaging from RV Knorr and the 12 kHz RV Knorr vertical echosounder line-transect measurements near Røst where RV Knorr tracks through the OAWRS imaged groups are given in (A) and corresponding line vertical echo-sounder data is given in (B-D). (E-H) Correspondence between OAWRS imaging and the 12 kHz RV Knorr vertical echosounder line-transect measurements taken 5 hours after OAWRS imaging near Røst. (I-L) Correspondence between OAWRS imaging and the 12 kHz RV Knorr vertical echosounder line-transect measurements taken roughly 24 hours after OAWRS imaging near Røst.

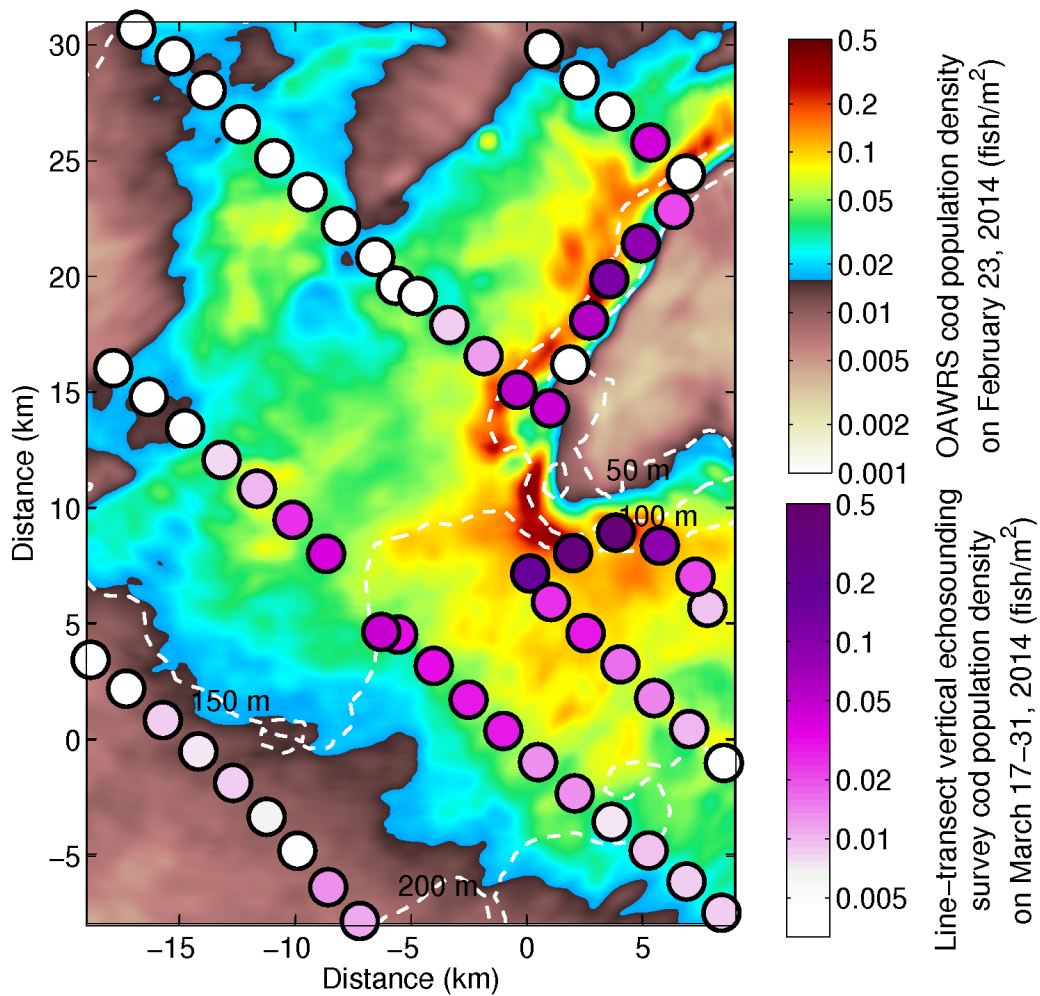


Figure S7: Consistency between cod population density distribution near Røst measured by OAWRS imaging on February 23, 2014 and by vertical echosounder measurements during the annual line-transect acoustic survey on March 17-31, 2014 (purple circles). High cod density areas near Røst and general tapering trends radially away from Røst are clear and consistent in both OAWRS and vertical echosounder measurements.

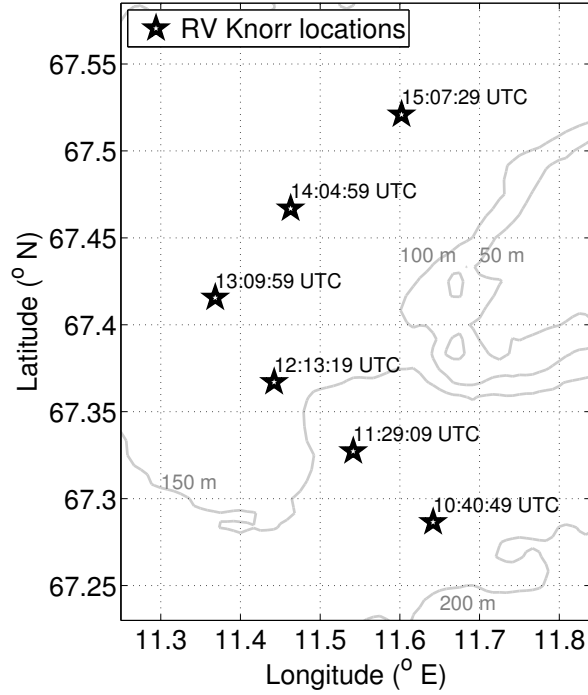


Figure S8: RV Knorr locations for the Fig. 1B mosaic at 10:40:49, 11:29:09, 12:13:19, 13:09:59, 14:04:59, and 15:07:29 UTC on February 23, 2014.

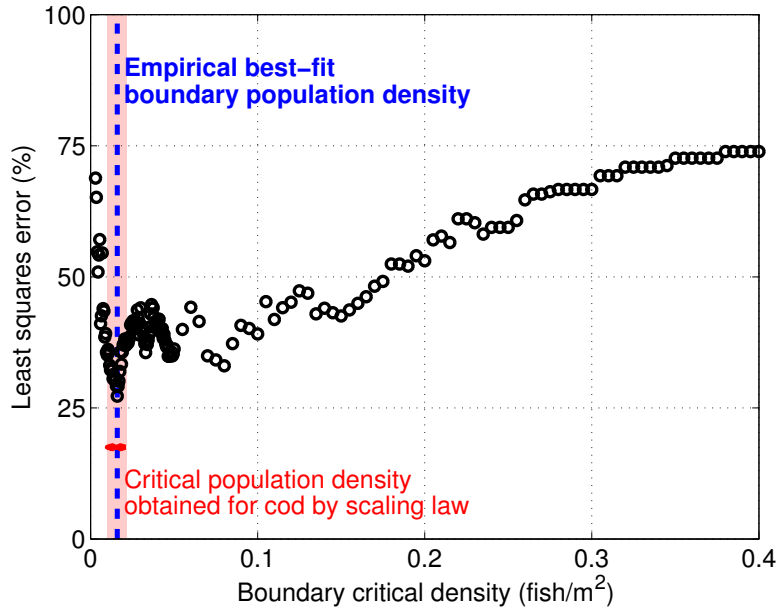


Figure S9: Least squares estimate of cod group boundary critical density from decades of North-east Arctic line-transect survey data and ICES spawning population time series. Cod group boundary critical density of roughly  $0.016 \text{ fish/m}^2$  is found to provide the lowest least squares error between the annual spawning population time series and decades of line-transect survey data under the assumption that summing spawning groups approximates the total annual spawning population each year from Eq.S2. Cod group boundary critical density range, in red, independently found from scaling herring critical density via Eq.S1 is consistent with this least squares result.

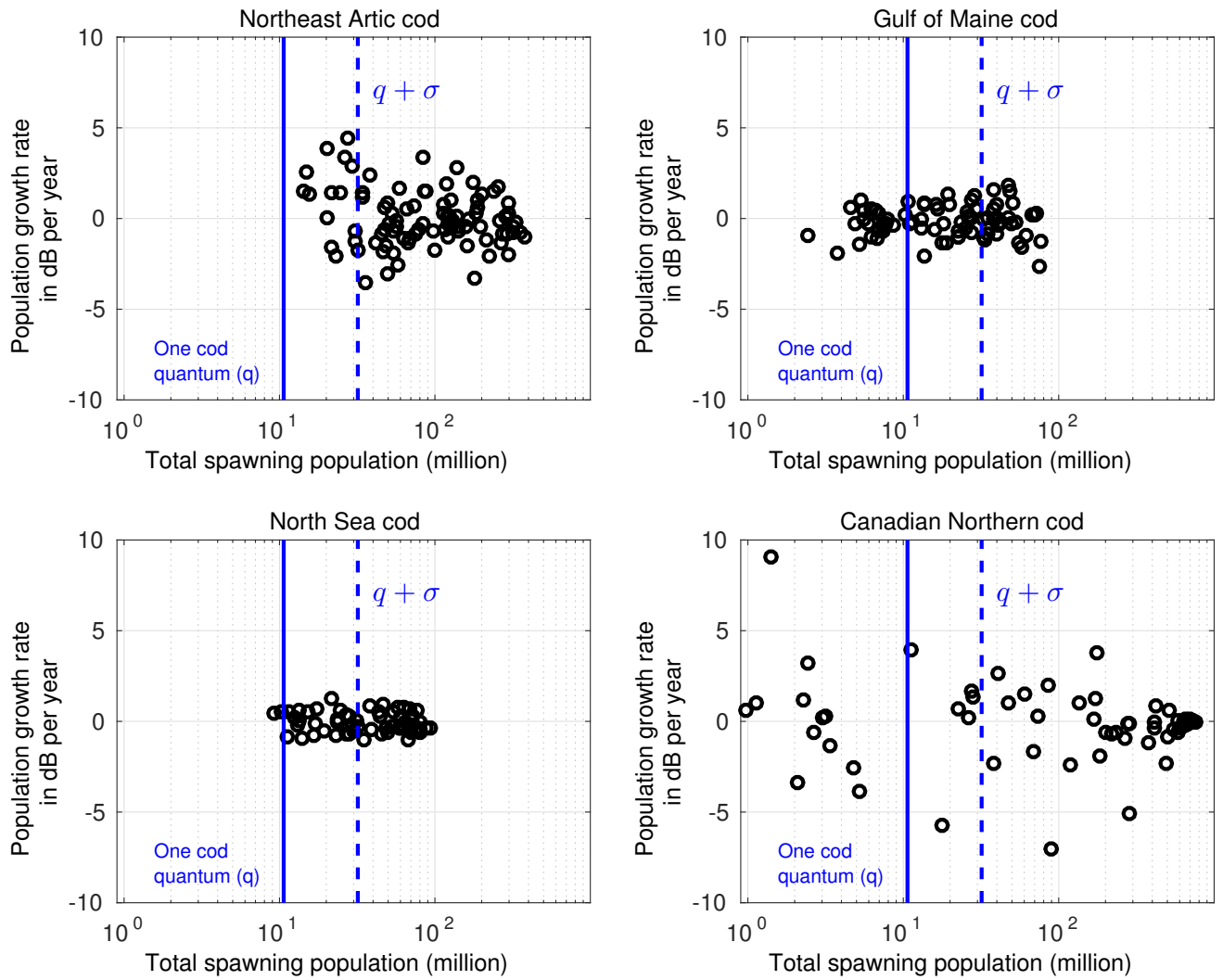


Figure S10: Population growth rate as a function of total spawning population each year from 1920 to 2014 for each cod population investigated. The cod quantum ( $q$ ) is the mean spawning groups size of 10.6 million with standard deviation ( $\sigma$ ) of 21.2 million found for Atlantic cod from a total population at pre-industrial levels, where the only available data was from the Northeast Arctic. The figures do not consistently show higher variance in growth rate for smaller populations.

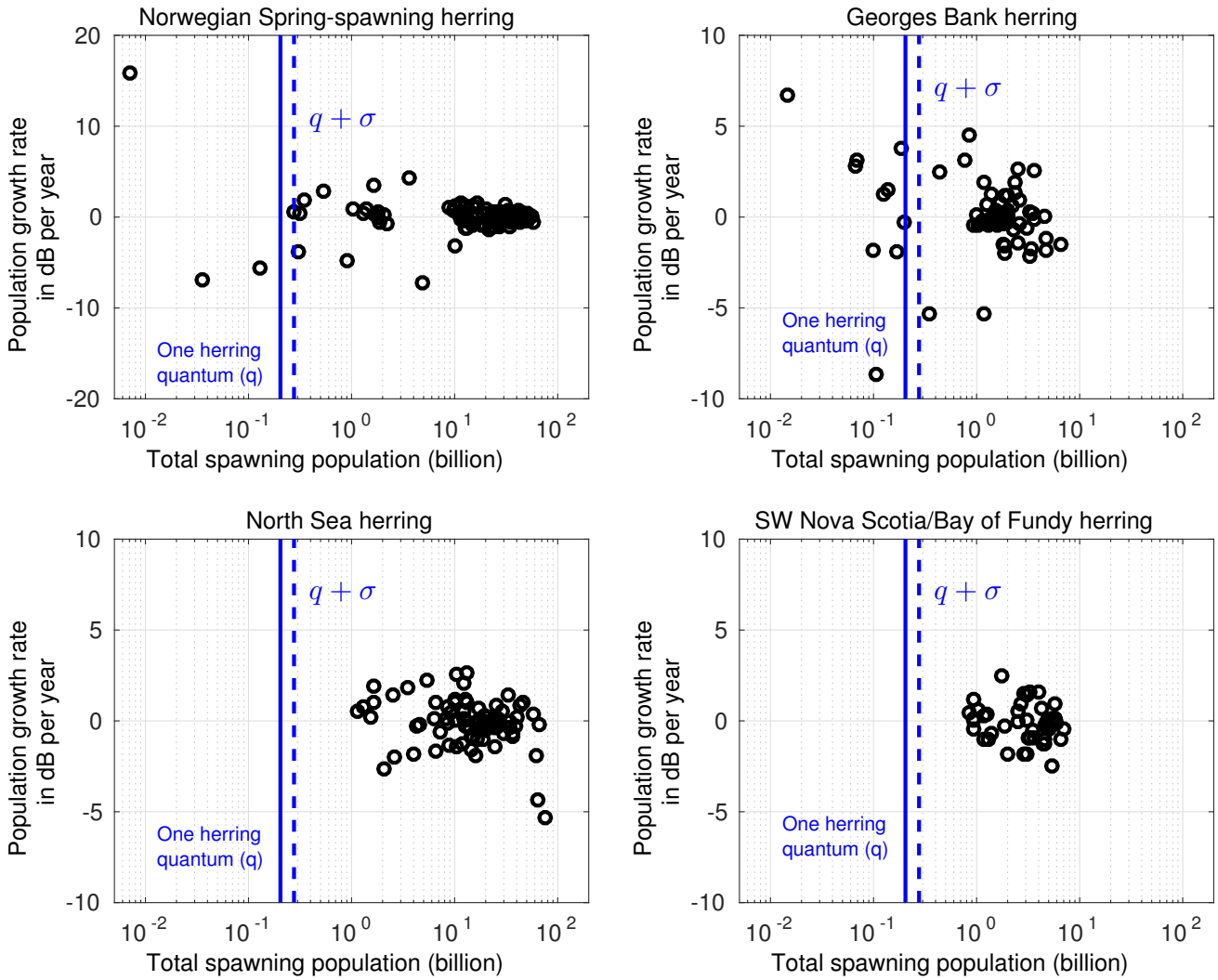


Figure S11: Population growth rate as a function of total spawning population each year from 1920 to 2014 for each herring population investigated. The herring quantum ( $q$ ) is the mean spawning groups size of 204 million with standard deviation ( $\sigma$ ) of 71.4 million found for Atlantic herring when the total population was at pre-industrial levels, where the only available data was from Georges Bank. The data show indications that for small populations below a standard deviation of a herring quantum, growth rate variance may be higher.